ACS OMEGA

Open Access

http://pubs.acs.org/journal/acsodf

Article

Synthesis and Biological Evaluation of a Novel Sugar-Conjugated Platinum(II) Complex Having a Tumor-Targeting Effect

Marina Omokawa, Hiroyuki Kimura,* Kenji Arimitsu, Yusuke Yagi, Yasunao Hattori, Hidekazu Kawashima, Yuki Naito, and Hiroyuki Yasui

Cite This: *ACS Omega* 2024, 9, 879−886

Read Online

ACCESS | Metrics & More | Article Recommendations | Supporting Information

ABSTRACT: We designed and synthesized a novel platinum complex conjugated with 2-fluorinated 2-deoxyglucoside, named FGC-Pt, to capitalize on the Warburg effect and metabolic trapping properties of [^{18}F]2-deoxy-2-fluoro-D-glucose ([^{18}F]FDG). Then, we conducted comprehensive in vitro and in vivo studies to evaluate the effects of FGC-Pt. In vitro cytotoxicity assays using HeLa cells revealed that FGC-Pt exhibited concentration-dependent cytotoxicity, even though its cytotoxic effect was less pronounced than that of cisplatin. In the evaluation of in vivo biodistribution in mice, platinum concentration in tumors and major organs (muscle, bone, blood, liver, and kidney) and the ratio of platinum concentration in tumors to major organs following the tail vein injection of FGC-Pt and cisplatin suggest that FGC-Pt is more retained in tumors than in other organs and tends to accumulate in tumors more than cisplatin. Furthermore, an in vivo assessment of the antitumor effect conducted in A549 cell-bearing mice demonstrated that FGC-Pt possesses substantial potential as an antitumor agent. It exhibited a tumor growth-inhibitory effect comparable to that of cisplatin while inducing lower toxicity, as evidenced by lower weight loss after administration. Herein, we successfully produced a novel compound with a tumor-growth-inhibitory effect comparable to that of cisplatin and low toxicity.

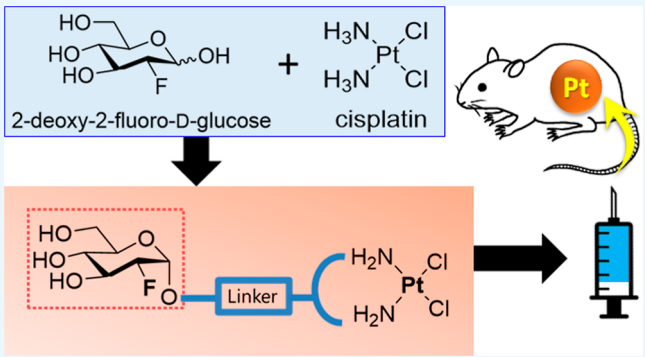

INTRODUCTION

Platinum-based antitumor drugs, such as cisplatin, carboplatin, and oxaliplatin, are widely used for the clinical treatment of various solid tumors.[1,2] Among them, cisplatin is used to treat patients with bladder, ovarian, head and neck, lung, testicular, cervical, esophageal, breast, and brain tumors, being widely effective against many types of cancers including carcinomas, germ cell tumors, lymphomas, and sarcomas. Therefore, cisplatin is one of the most commonly used drugs in clinical practice and is essential for cancer chemotherapy.[2−5]

Cisplatin, or *cis*-diamminedichloridoplatinum(II), is a platinum-coordination compound. It exhibits a square planar geometry characterized by two chloride ions in a cis orientation.[4] Cisplatin is a neutral metal complex with no net charge, easily traversing cell membranes.

As the chloride ion concentration is lower in cells than in plasma, water molecules replace the intracellular chloride ions coordinated to platinum, resulting in an active complex. The hydrolyzed product binds to the N7 position of purine residues in the nucleus, particularly, the guanine base. The formation of covalent adducts with deoxyribonucleic acid (DNA) damages DNA within the cancer cells, causing cell cycle arrest, blocking cell division, and leading to apoptotic cell death.[3−6] Additionally, mechanisms of action of cisplatin include the induction of DNA-damage-response-triggered apoptosis and mitochondrial apoptosis. Therefore, cisplatin exhibits anticancer activity through multiple mechanisms.[7−9] The interaction between cisplatin and DNA, leading to the formation of covalent adducts with purine bases, represents the basis for its effectiveness in cancer treatments. However, it is also the underlying cause of the cytotoxicity of cisplatin, resulting in various adverse effects, including nausea, nephrotoxicity, cardiotoxicity, hepatotoxicity, and neurotoxicity.[5] Thus, while existing platinum-based antitumor drugs are highly effective in treating cancer, their lack of tumor specificity and ability to induce severe adverse effects pose significant clinical challenges. Other platinum-based antitumor drugs, like cisplatin, also act through nonspecific mechanisms of action.[1] Therefore, the challenge lies in identifying tumor-specific targeting ligands to suppress the nonspecific distribution of platinum.[10]

Received: September 11, 2023
Revised: November 23, 2023
Accepted: December 5, 2023
Published: December 27, 2023

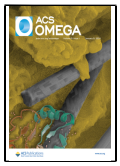

Cancer cells typically exhibit an altered glucose metabolism to survive in the hypoxic environment of malignant lesions. Unlike normal cells, they predominantly rely on glycolysis for energy production, whether oxygen is present or not. This process is known as aerobic glycolysis. Compared to oxidative phosphorylation, the process that normal cells adapt to under aerobic conditions, aerobic glycolysis yields much less adenosine triphosphate (ATP) from glucose. Consequently, highly proliferative cancer cells have a markedly increased requirement for glucose as their primary energy source, resulting in enhanced expression of glucose transporter membrane proteins (GLUTs) on the cell membrane surface and enhanced glucose uptake.[1,11−15] This phenomenon, later named the Warburg effect, has been recognized as a hallmark of cancer.[1,11−15] Among GLUT isoforms, GLUT1 is overexpressed in various cancers, and its overexpression in patient-derived tumor samples has been strongly correlated with poor prognosis, often marked by increased tumor invasiveness, rapid proliferation, and decreased patient survival.[12−17]

Therefore, since altered glucose intake and overexpression of glucose transporters are common in cancer, glucose transporters are clinically valid targets for cancer therapy.[17] The potential of glycoconjugates in both diagnosis and therapy is supported by the GLUT-mediated uptake and selective accumulation of the radioactive glucose derivative [^{18}F]2-deoxy-2-fluoro-D-glucose ([^{18}F]FDG) in cancer tissue.[17] Therefore, designing glycoconjugates that utilize sugar as a carrier for platinum-based drugs and target overexpressed glucose transporters holds promise for enhancing the selectivity of platinum-based drug design in tumor cells. This has led to active research into novel sugar-conjugated Pt (II) derivatives. The introduction of sugar chains into platinum complexes led to a substantial reduction in their toxicity and an improvement in their antitumor effects.[17−24] Moreover, [^{18}F]FDG is a diagnostic agent frequently used in clinical practice for the diagnosis, staging, and monitoring of various types of cancer.[25,26] After intravenous injection, [^{18}F]FDG enters cells via GLUT and is phosphorylated by hexokinase to form [^{18}F]FDG-6-phosphate. Normally, phosphorylated glucose undergoes intracellular metabolic processes such as glycolysis and glycogen formation, followed by the isomerization of glucose-6-phosphate to fructose-6-phosphate. Conversely, [^{18}F]FDG-6-phosphate lacks oxygen atoms at C-2 position, preventing further isomerization. As a result, [^{18}F]FDG-6-phosphate cannot diffuse out of the cell and undergoes dephosphorylation at a slow rate; therefore, it is "trapped" intracellularly, accumulating proportionally to the amount of glucose used.[12,27] This is known as metabolic trapping.

Based on the above-mentioned mechanism, the introduction of a fluorine atom at the 2-position of the sugar chain may enhance its retention in the tumor and improve its therapeutic effect. However, this concept has not been explored in previous drug design studies.

Hence, in this study, we aimed to address the issue of platinum-based antitumor drugs, which lack tumor specificity and often result in side effects. We sought to improve the therapeutic efficacy by increasing the intracellular retention within the tumor. To achieve this, we developed a novel sugar-linked platinum complex by exploiting the Warburg effect observed in cancer cells and capitalizing on the metabolic trapping characteristics of [^{18}F]FDG.

RESULTS AND DISCUSSION

Chemistry. When designing platinum complexes conjugated with 2-fluorinated 2-deoxyglucoside, we aimed to enhance the cellular uptake of platinum in tumors via the Warburg effect and increase its reactivity within cells by trapping metabolites such as 6-phosphorylated sugars. To achieve this, we considered introducing sugar on the non-leaving ligand side of platinum-based drugs, such as ammonia in cisplatin. Previous studies reported glucose-conjugated platinum complexes consisting of 2-glucopyranosidyl-1,3-propanediamine and two chloride ions as ligands.[24] Mikata et al.[28] also reported similar ligands in which 1,3-propanediamine was bound to various sugars. Thus, we planned to synthesize a platinum complex (FGC-Pt) comprising 1,3-propanediamine conjugated to 2-fluoro-2-deoxyglucose and two chloride ions (Scheme 1).

Scheme 1. Synthesis of FGC-Pt[a]

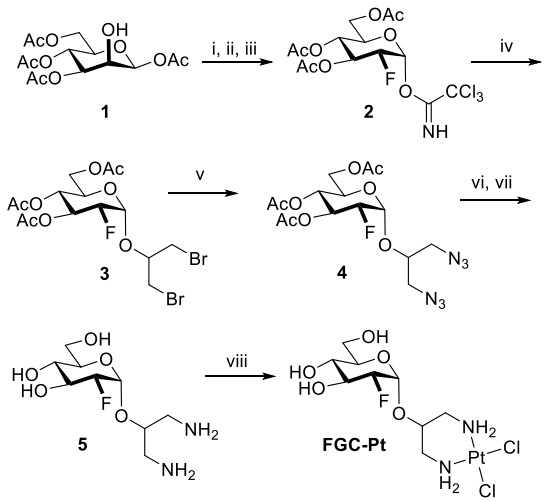

[a]Reagents and conditions: (i) DAST, 1,4-dioxane, 100 °C, 7 min, 78%; (ii) piperidine, THF, 24 °C, 4 h, 83%; (iii) CCl_3CN, DBU, CH_2Cl_2, 24 °C, 3 h, 76%; (iv) 1,3-dibromo-2-propanol, CH_2Cl_2, TMSOTf, 0 °C to rt, 22 h, 89%; (v) NaN_3, DMF, 30−70 °C, 6 h, 92%; (vi) NaOMe, MeOH, 24 °C, 2 h; (vii) Pd/C, MeOH, 24 °C, 2 h, 86%, 2 steps; (viii) $K_2[PtCl_4]$, H_2O, 24 °C, 24 h, 37%.

First, nucleophilic fluorination was performed using commercially available 1,3,4,6-tetra-*O*-acetyl-*β*-D-mannopyranose (**1**) as the starting material. Compound **S1** was then obtained. Subsequent steps involved deacetylation at position 1 and chloroimidation, resulting in the creation of imidate **2** as a glycosyl donor for glycosylation with 1,3-dibromopropan-2-ol. This step was necessary because glycosylation using an acetate substrate, as done in previous work by Mikata et al., did not proceed after 2-fluorination.

Subsequently, Schmidt's glycosylation with imidate **2** and 1,3-dibromopropan-2-ol was performed at 24 °C using trimethylsilyl trifluoromethanesulfonate (TMSOTf) as a promoter to produce compound **3**. Although Bucher et al. have also reported Schmidt's glycosylation using 2-fluorinated 2-deoxysugars, they reported that the use of 2-fluorinated 2-deoxyglucose at −30 °C gives a mixture of *α*- and *β*-isomers (*α*/*β* ratio is 1:1.9).[29] Conversely, under our conditions, only *α*-isomer could be obtained. We believe that this result is due to thermodynamic stereocontrol. Azidation of **3** resulted in the production of the diazido derivative **4**, followed by

https://doi.org/10.1021/acsomega.3c06922
ACS Omega 2024, 9, 879−886

deacetylation and subsequent reduction of the azido group to an amino group to obtain **5** as a diamine ligand for the platinum complex. Then, the complexation reaction of ligand **5** with $K_2[PtCl_4]$ resulted in the production of FGC-Pt in 37% yield.

FGC-Pt was purified by gel filtration using water. Although this complex is considered relatively stable in water, it was unexpectedly found that the chloride ion in FGC-Pt was easily replaced with acetonitrile when acetonitrile was used for high-performance liquid chromatography (HPLC) analysis.[30] The synthesized compounds were characterized by nuclear magnetic resonance (NMR) and electrospray ionization mass spectrometry (ESI-MS). The purity of FGC-Pt was determined to be 96% by quantitative (q)-NMR. The analysis revealed interesting changes in the ^{1}H NMR (400 MHz) and ^{13}C NMR (100 MHz) chemical shifts due to complexation. For example, the chemical shifts of the methylene hydrogens and carbons adjacent to the 1,3-propanediamine moiety coordinated with platinum shifted downfield (see Figure S18). However, the chemical shift of the methylene carbon at the γ-position from the nitrogen atom shifted upfield upon complexation (Figure S19). This upfield shift in the methylene carbon might be attributed to a steric compressive effect that is based on the Gauche relationship between Pt and the carbon at γ-position, which is shielded due to coordination.

Biology. *In Vitro Cytotoxicity Assay.* To identify the in vitro anticancer activity of FGC-Pt, we evaluated its cytotoxicity in comparison with that of cisplatin using a [3-(4,5-dimethylthiazol-2-yl)-5-(3-carboxymethoxyphenyl)-2-(4-sulfophenyl)-2H-tetrazolium] (MTS) assay with HeLa cells. Expression of GLUT1 was confirmed in HeLa cells by Western blotting analysis (see Figure S20). The corresponding half-maximal inhibitory concentration (IC_{50}) values are listed in Table 1, and photographs of the morphological changes in HeLa cells treated with FGC-Pt and cisplatin are shown in Figure 1. The IC_{50} value of cisplatin was 15.5 ± 2.3 μM. In addition, in the optical microscopy study, cisplatin-treated cells presented concentration-dependent morphological changes, and dead cells were conspicuous (Figure 1). Thus, cisplatin has a strong cytotoxic effect and exhibits cell-killing activity in a concentration-dependent manner. On the other hand, the IC_{50} value of FGC-Pt was 447.4 ± 99 μM, which is higher than that of cisplatin (Table 1). However, our optical microscopy observations and cell viability calculations based on absorbance measurements reveal that high concentrations of FGC-Pt can effectively induce cell death. These results indicate that FGC-Pt exhibits concentration-dependent cytotoxic activity and meets the basic requirements of an antitumor agent.

Table 1. Half-Maximal Inhibitory Concentration (IC_{50}) Values (μM) of Cisplatin and FGC-Pt in HeLa Cell Line[a]

compounds	IC_{50} (μM)
cisplatin	15.5 ± 2.3
FGC-Pt	447.4 ± 99

[a]Data are expressed as mean ± SD (n = 3).

In Vitro Stability of FGC-Pt in Mouse Plasma. To investigate the stability of FGC-Pt, FGC-Pt was mixed with mouse plasma and incubated at 37 °C. The results showed that 54.7 ± 5.7% of FGC-Pt was present at 2 h, with a half-life of approximately 2 h (Figure 2). This is longer than the 0.88 ± 0.05 h (mean ± SEM) half-life of cisplatin in plasma,[31] confirming its tendency to remain more stable than cisplatin in the plasma.

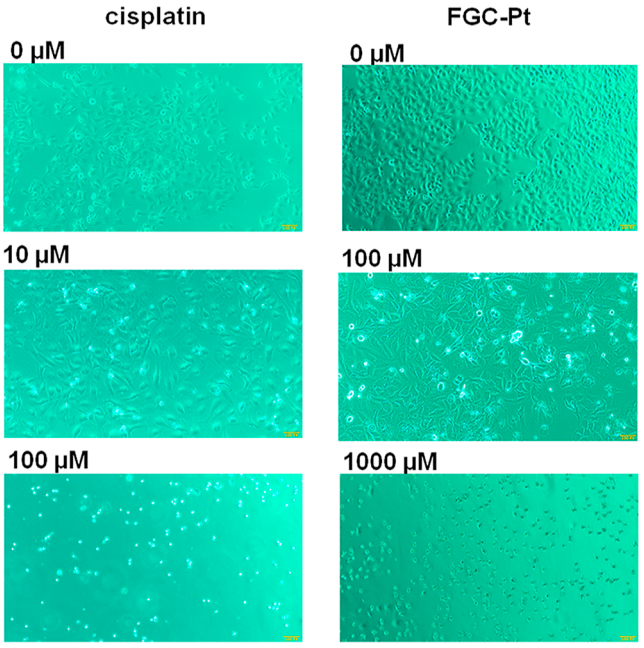

Figure 1. Observation of HeLa cells treated with cisplatin (0, 10, and 100 μM) and FGC-Pt (0, 100, and 1000 μM) by optical microscopy. (×100).

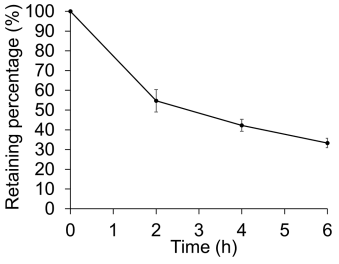

Figure 2. Stability of FGC-Pt in mouse plasma. Data are expressed as mean ± SD (n = 3).

In Vivo Biodistribution of FGC-Pt in Healthy Mice and A549 Cell-Bearing Mice. To investigate the basic characteristics of the biodistribution of FGC-Pt in healthy mice, the platinum concentration (expressed as Pt ng/g tissue) in 15 organs (pancreas, heart, lung, spleen, brain, muscle, bone, blood, gallbladder, stomach, small intestine, large intestine, liver, kidney, and thyroid) 24 h postinjection of FGC-Pt was analyzed by inductively coupled plasma mass spectrometry (ICP−MS) (Figure 3A). To confirm the accumulation and retentivity of FGC-Pt in tumors, we also assessed the platinum concentrations in major organs (muscle, bone, blood, liver, and kidney) and tumors in A549 cell-bearing mice at 24 and 48 h postinjection of FGC-Pt using ICP−MS (Figure 3B). In addition, we compared the distribution of FGC-Pt and cisplatin in A549 cell-bearing mice by analyzing the platinum concentration in major organs and tumors at 24 h post-injection of FGC-Pt and cisplatin using ICP−MS (Figure 3C). Although cisplatin is administered with large amounts of intravenous fluids during human treatment, this is not applicable in experiments on mice. Therefore, intravenous administration was selected as the method of administration in

https://doi.org/10.1021/acsomega.3c06922
ACS Omega 2024, 9, 879−886

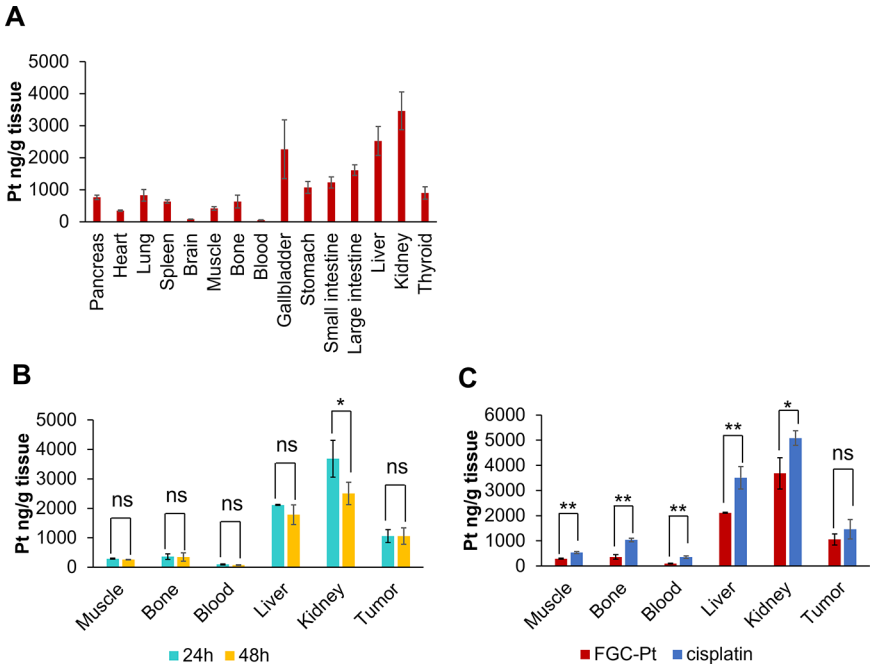

Figure 3. In vivo biodistribution of FGC-Pt and cisplatin. (A) Biodistribution of FGC-Pt in healthy mice 24 h after administration. Data are expressed as mean ± SD (n = 6). (B) Biodistribution in A549 cell-bearing mice at 24 and 48 h postinjection of FGC-Pt. (C) Comparison of biodistribution in A549 cell-bearing mice 24 h postinjection of FGC-Pt and cisplatin. Data are expressed as mean ± SD (n = 4). The statistical significance of the difference among groups was determined by Student's t-test. (Significance: *p < 0.05, **p < 0.01, ns: not significant).

our study in order to reflect clinical conditions as closely as possible, despite this condition being likely to cause cisplatin toxicity. To compare the intratumor accumulation rates of FGC-Pt and cisplatin and examine changes in the intratumor accumulation rate of FGC-Pt over time, we calculated the ratios of platinum concentration in tumors to major organs at 24 and 48 h postinjection of FGC-Pt, as well as at 24 h postinjection of cisplatin (Table 2). Expression of GLUT1 was confirmed in A549 cells by Western blotting analysis (Figure S20).

Table 2. Ratio of Platinum Concentration in Tumors to Other Major Organs (Muscle, Bone, Blood, Liver, and Kidney) at 24 and 48 h Post-Injection of FGC-Pt and 24 h Post-Injection of Cisplatin in A549 Cell-Bearing Mice

	value of the ratio				
	tumor/ muscle	tumor/ bone	tumor/ blood	tumor/ liver	tumor/ kidney
FGC-Pt (24 h)	3.64	2.93	11.07	0.50	0.29
FGC-Pt (48 h)	4.09	3.03	14.37	0.59	0.42
cisplatin (24 h)	2.72	1.41	4.10	0.42	0.29

Platinum accumulation in tumors at 24 and 48 h post-FGC-Pt injection (24 h: 1058 ± 220 Pt ng/g tissue, 48 h: 1055 ± 278 Pt ng/g tissue) was confirmed, and no significant difference was found between the two values (Figure 3B). In addition, the ratios of Pt content in tumors to major organs at 24 and 48 h post-FGC-Pt injection increased over time (Table 2). These results suggest that the elimination of platinum from tumors was slower compared to other organs in FGC-Pt-treated A549 cell-bearing mice, possibly due to enhanced metabolic trapping in tumors. We then measured the platinum concentration in the organs 24 h postinjection of FGC-Pt and cisplatin, finding high values in all organs for both compounds (Figure 3C). There was no significant difference between FGC-Pt and cisplatin in the accumulation of platinum in tumors. However, platinum accumulation in other organs at 24 h postinjection of FGC-Pt was lower than that of cisplatin (*p < 0.05, **p < 0.01; Figure 3C). In addition, the ratios of Pt in tumors to other organs except for tumor-to-kidney (tumor/kidney) ratios were higher for FGC-Pt in all cases (Table 2). These results indicate that FGC-Pt tends to accumulate in tumors more readily than cisplatin. The platinum concentration in the kidney 24 and 48 h post-FGC-Pt injection decreased significantly over time (*p < 0.05; Figure 3B). This suggests that FGC-Pt is not retained in the kidney and is excreted by the kidney. The nephrotoxicity of platinum-based antitumor drugs is known to depend on the amount of platinum accumulation in the kidney.[32] Therefore, FGC-Pt has the potential to avoid nephrotoxicity caused by platinum accumulation in the kidney. Additionally, the higher tumor-to-bone (tumor/bone) ratio of FGC-Pt compared to that of cisplatin suggests a potential reduction in bone marrow suppression (Table 2).

In Vivo Assessment of the Antitumor Effect of FGC-Pt and Cisplatin Using A549 Cell-Bearing Mice. To investigate the in vivo antitumor effect of FGC-Pt, A549 cell-bearing mice were treated on days 1, 8, 15, and 22 with saline, FGC-Pt (2.7 mg of Pt/kg), or cisplatin (2.7 mg of Pt/kg) via intravenous injection. The antitumor effect was evaluated by measuring the tumor volume over 30 days. Furthermore, the toxic side effects of these platinum complexes were assessed by examination of the animals, including body weight, signs of lethargy, loss of appetite, and condition of the injection site. As shown in Figure 4A, the FGC-Pt-treated group exhibited similar tumor growth inhibition as the cisplatin-treated group, with no significant difference in tumor size (Figure 4A). Furthermore, although null hypotheses were retained by Tukey's all-pairwise comparison, these groups presented a trend toward greater

https://doi.org/10.1021/acsomega.3c06922
ACS Omega 2024, 9, 879−886

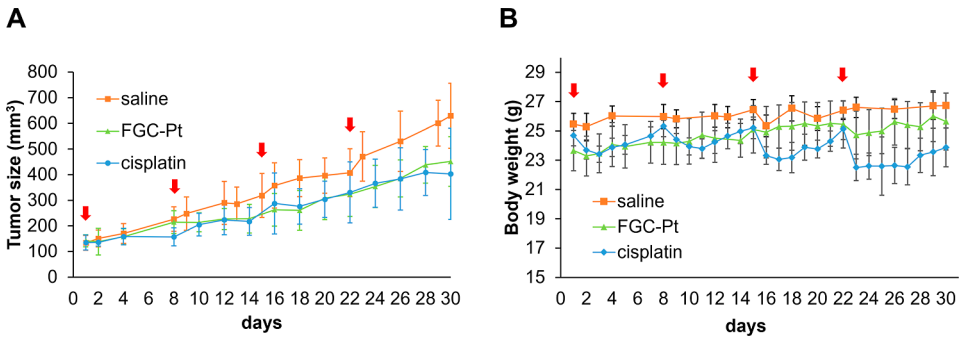

Figure 4. In vivo antitumor effect of FGC-Pt in A549 cell-bearing mice.

tumor growth inhibition than the saline-treated group (Figure 4A). However, the cisplatin-treated group experienced a more pronounced weight loss after the fourth dose (administered on days 1, 8, 15, and 22) than the FGC-Pt-treated group (Figure 4B). Additionally, a higher number of mice in the cisplatin-treated group exhibited loss of appetite and presented with a red and swollen injection site compared to those treated with FGC-Pt. These results indicate that FGC-Pt reduces toxicity compared to that of cisplatin but has comparable effects on tumor growth.

Mice were randomly divided into three groups: saline group (n = 6), FGC-Pt group (n = 6), and cisplatin group (n = 6). They were treated on days 1, 8, 15, and 22 with saline, FGC-Pt (2.7 mg of Pt/kg), or cisplatin (2.7 mg of Pt/kg) via intravenous injection. (A) Tumor growth over time in A549 cell-bearing mice treated with saline, FGC-Pt, or cisplatin. (B) Toxicity assessment of saline, FGC-Pt, and cisplatin by monitoring body weight in A549 cell-bearing mice. Data are expressed as mean ± SD (n = 6). The statistical significance of differences among groups was determined by Tukey's test.

CONCLUSIONS

To harness the Warburg effect in cancer cells and exploit the metabolic trapping properties of [^{18}F]FDG, we designed and synthesized a novel sugar-conjugated platinum(II) complex incorporating 2-fluorinated 2-deoxyglucoside inspired by cisplatin.

In vitro evaluation of cytotoxicity demonstrated that FGC-Pt does not possess the same level of cytotoxicity as that of cisplatin. However, it does display concentration-dependent cell-killing activity, similar to cisplatin. In addition, approximately 55% of FGC-Pt was present in mouse plasma after 2 h, and the half-life of FGC-Pt was approximately 2 h. In the evaluation of biodistribution, platinum accumulation in tumors at 24 and 48 h postinjection of FGC-Pt showed no significant difference in those values. Furthermore, the changes in the ratio of platinum concentration in tumors to other major organs following administration of FGC-Pt indicated that FGC-Pt is more retained in tumors. Additionally, the ratios of Pt in tumors compared to other organs at 24 h postinjection of FGC-Pt and cisplatin and a comparison of the biodistribution of these compounds indicated that FGC-Pt tends to accumulate in tumors more readily than cisplatin. Furthermore, despite being less toxic than cisplatin, FGC-Pt demonstrated a tumor growth-inhibitory effect as effective as that of cisplatin when compared to the control groups.

These results suggest the potential of FGC-Pt as an antitumor drug, but the detailed mechanism of cellular uptake of FGC-Pt is under study. In addition, the strategy outlined in this study holds promise for the future development of new sugar-based platinum complexes. In this study, although we have not yet been able to validate a strategy using the Warburg effect, we hope to build up a drug discovery platform using established synthetic methods and aim to develop anticancer drugs that selectively accumulate in tumors.

MATERIALS AND METHODS

General Information. All reagents, solvents, and starting materials were purchased from commercial sources: Tokyo Chemical Industry Co., Ltd. (Tokyo, Japan), Nacalai Tesque Inc. (Kyoto, Japan), and Fujifilm Wako Pure Chemical Corporation (Osaka, Japan), and used without further purification. NMR spectra were obtained using a Bruker Ascend 500 NMR spectrometer (Bruker, Billerica, MA, USA) and a JEOL JNM ECS-400 spectrometer (JEOL, Tokyo, Japan). ^{1}H NMR spectra were collected at 400 or 500 MHz, and ^{13}C NMR spectra were collected at 125 or 100 MHz. ^{1}H NMR chemical shifts (δ) are shown in parts per million (ppm) relative to tetramethylsilane (0 ppm), which was used as the internal standard. ^{1}H NMR showed chemical shifts based on the solvent peak (4.75 ppm) when D_2O was used. The ^{13}C NMR values were reported relative to tetramethylsilane (0 ppm) or 3-(trimethylsilyl)propionic-2,2,3,3-d_4-acid sodium salt (0 ppm), which was used as an internal standard. Assignments were based on the analysis of coupling constants as well as correlation spectroscopy, heteronuclear single quantum coherence, and heteronuclear multiple bond correlation spectra. High-resolution mass spectra were obtained by using an LC-MS-IT-TOF instrument (Shimadzu, Kyoto, Japan). Chromatographic purification was performed using an EPCLC W-Prep 2XY automated flash chromatography system (Yamazen Corp., Osaka, Japan). Thin-layer chromatography (TLC) was performed on silica gel 60 F_{254} plates (Merck, Darmstadt, Germany) and NH_2 silica gel 60 F_{254} plates (Wako Pure Chemical Industries). Platinum concentration was determined using ICP−MS (Agilent 7700X ICP−MS, Agilent Technologies, Tokyo, Japan). Analytical HPLC was performed using a Shimadzu LD-20AD (Shimadzu Corporation, Kyoto, Japan) fitted with a Sugar-D column (4.6 ID × 150 mm) (Nacalai Tesque Inc.) and an SPD-20A (Shimadzu Corporation) UV detector. The flow rate was 0.5 mL/min, and UV absorption was measured at 220 nm. The runs were performed with linear gradients of Millipore water (A) and methanol (B; FujifilumWako HPLC-grade): t = 0−7 min, 85% B; t = 7−10 min, 85−50%, t = 10−30 min, 50−10% B. All animal care and experimental studies were performed in accordance with the guidelines and with the approval of the Animal Investigation Committee of Kyoto Pharmaceutical University.

https://doi.org/10.1021/acsomega.3c06922
ACS Omega 2024, 9, 879−886

Synthesis of Compounds. *1,3,4,6-Tetra-O-acetyl-2-deoxy-2-fluoro-β-D-glucopyranose (S1).* 1,3,4,6-Tetra-*O*-acetyl-β-D-mannopyranose (**1**) (2.00 g, 5.74 mmol) was reacted with DAST (2.30 mL, 17.2 mmol) in 1,4-dioxane (40.0 mL) under N_2 atmosphere. After being stirred at 100 °C for 7 min, the reaction mixture was cooled to 0 °C, and methanol (6.60 mL) was added. The reaction mixture was diluted with chloroform and washed thrice with saturated aqueous sodium bicarbonate and brine. The organic layer was dried over anhydrous magnesium sulfate and evaporated in vacuo. The residue was purified by silica gel chromatography (hexane/ethyl acetate = 1:1) to obtain **S1** (1.57 g, 78%).

3,4,6-Tri-O-acetyl-2-deoxy-2-fluoro-α-D-glucopyranosyl Trichloroacetimidate (2). Compound **S1** (2.77 g, 7.91 mmol) was reacted with piperidine (4.55 mL, 45.9 mmol) in THF (55.4 mL) under N_2 atmosphere. The solution was stirred at 24 °C for 4 h. After completing the reaction, the mixture was poured into 1% hydrochloric acid and extracted using ethyl acetate. The organic layer was washed with brine, dried over anhydrous sodium sulfate, and evaporated in vacuo. The crude product was purified by silica gel chromatography (hexane/ethyl acetate = 1:1) yielding 3,4,6-tri-*O*-acetyl-2-deoxy-2-fluoro-D-glucopyranose (2.02 g, 83%) as a mixture of α and β anomers (α/β anomer ratio = 71:29). CCl_3CN (3.60 mL, 35.5 mmol) and DBU (3.60 mL, 35.5 mmol) were added to a solution of 3,4,6-tri-*O*-acetyl-2-deoxy-2-fluoro-D-glucopyranose (1.99 g, 6.45 mmol) in CH_2Cl_2 (40.0 mL) under N_2 atmosphere. The resulting solution was stirred at 24 °C for 1.5 h. The reaction was quenched with water, and the mixture was extracted with ethyl acetate. The organic layer was washed with brine, dried over anhydrous magnesium sulfate, and evaporated in vacuo. The crude product was purified using silica gel chromatography (hexane/ethyl acetate = 2:1) to yield **2** (2.23 g, 76%).

1,3-Dibromo-2-propyl 3,4,6-Tri-O-acetyl-2-deoxy-2-fluoro-α-D-glucopyranoside (3). 1,3-Dibromo-2-propanol (55.6 μL, 0.54 mmol) and TMSOTf (19.5 μL, 0.108 mmol) were added to a solution of compound **2** (98.5 mg, 0.217 mmol) in CH_2Cl_2 (2.00 mL) under Ar atmosphere. The solution was stirred for 22 h, gradually returning to 24 °C from 0 °C. After completion of the reaction, the reaction was quenched with a saturated aqueous solution of sodium bicarbonate, and the mixture was extracted with ethyl acetate. The organic layer was washed with brine, dried over anhydrous sodium sulfate, and evaporated in vacuo. The crude product was purified using amino silica gel chromatography (hexane/ethyl acetate = 2:1) to yield compound **3** (97.1 mg, 88%).

1,3-Diazido-2-propyl 3,4,6-Tri-O-acetyl-2-deoxy-2-fluoro-α-D-glucopyranoside (4). A solution of compound **3** (1.71 g, 3.37 mmol) in DMF (34.0 mL) was reacted with NaN_3 (2.65 g, 40.5 mmol) under N_2 atmosphere. The resulting solution was stirred at 70 °C for 6 h. The reaction was quenched with water, and the mixture was extracted with ethyl acetate. The organic layer was washed five times with water, dried over anhydrous magnesium sulfate, and evaporated in vacuo. The crude product was purified using silica gel chromatography (hexane/ethyl acetate = 2:1) to yield **4** (1.34 g, 92%).

1,3-Diamino-2-propyl 2-Deoxy-2-fluoro-α-D-glucopyranoside (5). A solution of compound **4** (1.34 g, 3.45 mmol) in MeOH (27.0 mL) was added to NaOMe (28% in methanol, ca. 0.8 mL) under N_2 atmosphere. The mixture was stirred at 24 °C for 2 h. The resulting solution was neutralized using a Dowex 50 W-X4 200−400 MESH HFORM. After filtration to remove the resin (washing with MeOH), the filtrate was evaporated in vacuo to give 1,3-diazido-2-propyl 2-deoxy-2-fluoro-α-D-glucopyranoside (987 mg, 93%). Compound **S3** was used in subsequent reactions without purification. Palladium-activated carbon (10% Pd, 98.2 mg) was added to a solution of compound **S3** (935 mg, 3.05 mmol) in methanol (20.0 mL), and the mixture was stirred under H_2 atmosphere at 24 °C for 2 h. The resulting solution was filtered through a Hyflo Super-Cel layer, and the filtrate was evaporated in vacuo to obtain **5** (703 mg, 91%).

cis-Dichloro [(2-Fluoro-α-D-glucopylanosidyl)propane-1,3-diamine] Platinum (6): FGC-Pt. $K_2[PtCl_4]$ (257 mg, 0.620 mmol) was added to a solution of **5** (155 mg, 0.610 mmol) in water (3.10 mL). The mixture was stirred in the dark under N_2 atmosphere at 24 °C for 24 h. The resulting solution was purified using a Biogel P2 resin column. Based on SiO_2-TLC monitoring (isopropanol/water/aqueous ammonium solution = 6:5:2, R_f = 0.77), the fractions were combined and evaporated in vacuo to yield **6** (116 mg, 37%).

Cell Culture. HeLa (human cervical cancer) and A549 (human lung cancer) cell lines were purchased from the European Collection of Authenticated Cell Cultures (ECACC, London, UK). HeLa cells were cultured in Eagle's minimum essential medium (Fujifilm Wako Pure Chemical Corporation) containing 10% fetal bovine serum (Sigma-Aldrich, St. Louis, MO, USA), 1% penicillin−streptomycin (Nacalai Tesque Inc.), nonessential amino acids solution 1 mM (Nacalai Tesque Inc.), and 1% sodium pyruvate solution (Nacalai Tesque Inc.) in a humidified atmosphere containing 5% CO_2 at 37 °C. A549 cells were cultured in Ham's F-12K medium (Fujifilm Wako Pure Chemical Corporation) containing 10% fetal bovine serum (Sigma-Aldrich) and 1% penicillin−streptomycin (Nacalai Tesque Inc.) in a humidified atmosphere containing 5% CO_2 at 37 °C. The cells were passaged twice a week until reaching 70−90% confluence.

In Vitro Cytotoxicity Assay. HeLa cells were seeded in 24-well plates (Corning, New York, USA) at 40000 cells/well and incubated in 5% CO_2 atmosphere in 1 mL of complete medium at 37 °C for 24 h. Subsequently, 500 μL of freshly prepared culture medium containing drugs at multiple concentrations (cisplatin:0−100 μM, FGC-Pt:0−1000 μM) was added, and incubated for another 48 h. MTS reagent (Promega Corporation, Madison, WI, USA) was added, and the cells were incubated for 3 h. Finally, 100 μL of the medium containing MTS was transferred to 96-well plates (AGC TECHNO GLASS Co., Ltd., Shizuoka, Japan). The absorbance was measured at 490 nm. IC_{50} values were calculated using GraphPad Prism software (version 6.00 for Windows; GraphPad, Inc., California, USA). All experiments were performed in triplicate.

In Vitro Stability of FGC-Pt in Mouse Plasma. Plasma was purchased from Japan SLC (Shizuoka, Japan). FGC-Pt (2.4 mg) was mixed with plasma (160 μL) and incubated at 37 °C. The mixtures were incubated at 37 °C for 0, 2, 4, and 6 h, mixed with saline, and filtrated using a syringe filter (Nacalai Tesque Inc.). The filtrate was analyzed by HPLC. HPLC analysis was carried out under the aforementioned measurement conditions.

Biodistribution of FGC-Pt and Cisplatin in Healthy Mice and A549 Cell-Bearing Mice. The in vivo biodistribution of FGC-Pt was evaluated in healthy and A549 cell-bearing mice. Five-week-old male BALB/c nu/nu mice were purchased from Japan SLC (Shizuoka, Japan) and

https://doi.org/10.1021/acsomega.3c06922
ACS Omega 2024, 9, 879−886

quarantined for 1 week prior to tumor inoculation. A549 cells were injected subcutaneously into the right shoulder at a concentration of 1×10^7 cells/site. Tumor volume was calculated using the following formula: $V = (4/3) \times \pi \times$ (tumor length/2) × (tumor width/2) × (tumor height/2). Five-week-old male Slc/ddy mice were purchased from Japan SLC (Shizuoka, Japan) and quarantined for 1 week prior to drug injection. The experiment began when the tumor size reached 50 mm^3. Freshly prepared saline solutions of 4 mg of Pt/kg of FGC-Pt and cisplatin were administered by tail vein injections to healthy mice (n = 6/group) and A549 cell-bearing mice (n = 4/group). Biodistribution was assessed by ICP−MS at 24 and 48 h postinjection of the tested drugs. Quantification of the platinum concentration was performed by ICP−MS after nitric acid, perchloric acid, and hydrogen acid digestion.

In Vivo Assessment of the Antitumor Effect of FGC-Pt and Cisplatin Using A549 Cell-Bearing Mice. Five-week-old male BALB/c nu/nu mice were purchased from Japan SLC (Shizuoka, Japan) and quarantined for 1 week prior to tumor inoculation. A549 cells were subcutaneously injected at a concentration of 1×10^7 cells/site into the right shoulder. The experiment began when the tumors reached 100−200 mm^3 in size. The mice were randomly divided into three groups: control (saline, 4.0 mL/kg, n = 6), FGC-Pt (2.7 mg of Pt/kg, n = 6), and cisplatin (2.7 mg of Pt/kg, n = 6). FGC-Pt and cisplatin were freshly prepared by dissolution in saline before injection and administered via tail vein injection on days 1, 8, 15, and 22. The mice were weighed, and their weight was recorded.

Statistical Analysis. Data are expressed as means ± standard deviation (SD), and BellCurve for Excell (version 3.21) (Social Survey Research Information Co., Ltd., Tokyo, Japan) was used for all statistical analyses. Student's t-test was used for two-group comparisons. Multiple comparisons among groups were performed using Tukey's test. Differences were considered significant when $p < 0.05$.

■ ASSOCIATED CONTENT

Supporting Information

The Supporting Information is available free of charge at https://pubs.acs.org/doi/10.1021/acsomega.3c06922.

Method of Western blotting analysis, characterization date of compounds, HR-MS and NMR spectra of compounds, comparison of ^{1}H NMR spectra of compound **5** and FGC-Pt, comparison of ^{13}C NMR spectra of compound **5** and FGC-Pt, and expression of GLUT1 in HeLa cells and A549 cells (PDF)

■ AUTHOR INFORMATION

Corresponding Author

Hiroyuki Kimura − *Laboratory of Analytical and Bioinorganic Chemistry, Division of Analytical and Physical Sciences, Kyoto Pharmaceutical University, Kyoto 607-8414, Japan; Division of Probe Chemistry for Disease Analysis/ Central Institute for Radioisotope Science, Research Center for Experimental Modeling of Human Disease, Kanazawa University, Kanazawa 920-8640, Japan;* orcid.org/0000-0002-4291-3524; Email: hkimura@staff.kanazawa-u.ac.jp

Authors

Marina Omokawa − *Laboratory of Analytical and Bioinorganic Chemistry, Division of Analytical and Physical Sciences, Kyoto Pharmaceutical University, Kyoto 607-8414, Japan*

Kenji Arimitsu − *Laboratory of Analytical and Bioinorganic Chemistry, Division of Analytical and Physical Sciences, Kyoto Pharmaceutical University, Kyoto 607-8414, Japan; Laboratory of Medicinal Chemistry, Faculty of Pharmacy, Osaka Ohtani University, Tondabayashi, Osaka 584-8540, Japan;* orcid.org/0000-0003-2844-1652

Yusuke Yagi − *Laboratory of Analytical and Bioinorganic Chemistry, Division of Analytical and Physical Sciences, Kyoto Pharmaceutical University, Kyoto 607-8414, Japan; Department of Radiological Technology, Faculty of Medicinal Science, Kyoto College of Medical Science, Nantan 622-0041 Kyoto, Japan;* orcid.org/0000-0003-0937-3746

Yasunao Hattori − *Center for Instrumental Analysis, Kyoto Pharmaceutical University, Kyoto 607-8412, Japan*

Hidekazu Kawashima − *Radioisotope Research Center, Kyoto Pharmaceutical University, Kyoto 607-8412, Japan*

Yuki Naito − *Laboratory of Analytical and Bioinorganic Chemistry, Division of Analytical and Physical Sciences, Kyoto Pharmaceutical University, Kyoto 607-8414, Japan*

Hiroyuki Yasui − *Laboratory of Analytical and Bioinorganic Chemistry, Division of Analytical and Physical Sciences, Kyoto Pharmaceutical University, Kyoto 607-8414, Japan*

Complete contact information is available at: https://pubs.acs.org/10.1021/acsomega.3c06922

Author Contributions

M.O. and H.K. designed the study. All authors performed analyses in the data and results.

Funding

This work was supported by a Private University Research Branding Project for the Ministry of Education, Culture, Sports, Science, and Technology, and JSPS KAKENHI with grant no. JP17K19670, JP17K10377, 22H02928.

Notes

The authors declare no competing financial interest.

■ ACKNOWLEDGMENTS

We thank Dr. Saito Michiko of Kyoto Pharmaceutical University, Bioscience Research Center, for her support with in vivo experiments.

■ ABBREVIATIONS

DAST, *N*,*N*-diethylaminosulfur trifluoride; THF, tetrahydrofuran; CCl_3CN, trichloroacetonitrile; DBU, 1,8-diazabicyclo-[5,4,0]-7-undecene; CH_2Cl_2, dichloromethane; NaN_3, sodium azide; DMF, *N*,*N*-dimethylformamide; NaOMe, sodium methoxide; MeOH, methanol; Pd/c, palladium on carbon; $K_2[PtCl_4]$, potassium tetrachloroplatinate (II); PBS, phosphate-buffered saline; HR-MS, high-resolution mass spectrometry

■ REFERENCES

(1) Wang, X.; Guo, Z. Targeting and Delivery of Platinum-Based Anticancer Drugs. *Chem. Soc. Rev.* **2013**, *42*, 202−224.

(2) Johnstone, T. C.; Suntharalingam, K.; Lippard, S. J. The Next Generation of Platinum Drugs: Targeted Pt(II) Agents, Nanoparticle Delivery, and Pt(IV) Prodrugs. *Chem. Rev.* **2016**, *116*, 3436−3486.

(3) Ghosh, S. Cisplatin: The first metal based anticancer drug. *Bioorg. Chem.* **2019**, *88*, 102925.

(4) Dasari, S.; Bernard Tchounwou, P. Cisplatin in Cancer Therapy: Molecular Mechanisms of Action. *Eur. J. Pharmacol.* **2014**, *740*, 364−378.
(5) Aldossary, S. A. Review on Pharmacology of Cisplatin: Clinical Use, Toxicity and Mechanism of Resistance of Cisplatin. *Biomed. Pharmacol. J.* **2019**, *12*, 07−15.
(6) Tchounwou, P. B.; Dasari, S.; Noubissi, F. K.; Ray, P.; Kumar, S. Advances in Our Understanding of the Molecular Mechanisms of Action of Cisplatin in Cancer Therapy. *J. Exp. Med.* **2021**, *13*, 303−328.
(7) Galluzzi, L.; Senovilla, L.; Vitale, I.; Michels, J.; Martins, I.; Kepp, O.; Castedo, M.; Kroemer, G. Molecular Mechanisms of Cisplatin Resistance. *Oncogene* **2012**, *31*, 1869−1883.
(8) Jamieson, E. R.; Lippard, S. J. Structure, Recognition, and Processing of Cisplatin-DNA Adducts. *Chem. Rev.* **1999**, *99*, 2467−2498.
(9) Cohen, S. M.; Lippard, S. J. Cisplatin: From DNA Damage to Cancer Chemotherapy. *Prog. Nucleic Acid Res. Mol. Biol.* **2001**, *67*, 93−130.
(10) Cho, H.-J.; Park, S.-J.; Lee, Y.-S.; Kim, S. Theranostic iRGD Peptide Containing Cisplatin Prodrug: Dual-Cargo Tumor Penetration for Improved Imaging and Therapy. *J. Controlled Release* **2019**, *300*, 73−80.
(11) Vander Heiden, M. G.; Cantley, L. C.; Thompson, C. B. Understanding the Warburg Effect: The Metabolic Requirements of Cell Proliferation. *Science* **2009**, *324*, 1029−1033.
(12) Szablewski, L. Expression of Glucose Transporters in Cancers. *Biochim. Biophys. Acta* **2013**, *1835*, 164−169.
(13) Macheda, M. L.; Rogers, S.; Best, J. D. Molecular and Cellular Regulation of Glucose Transporter (GLUT) Proteins in Cancer. *J. Cell. Physiol.* **2005**, *202*, 654−662.
(14) Barron, C. C.; Bilan, P. J.; Tsakiridis, T.; Tsiani, E. Facilitative Glucose Transporters: Implications for Cancer Detection, Prognosis and Treatment. *Metabolism* **2016**, *65*, 124−139.
(15) Ancey, P. B.; Contat, C.; Meylan, E. Glucose Transporters in Cancer - From Tumor Cells to the Tumor Microenvironment. *FEBS J.* **2018**, *285*, 2926−2943.
(16) Zambrano, A.; Molt, M.; Uribe, E.; Salas, M. Glut 1 in Cancer Cells and the Inhibitory Action of Resveratrol as A Potential Therapeutic Strategy. *J. Mol. Sci.* **2019**, *20* (13), 3374.
(17) Patra, M.; Awuah, S. G.; Lippard, S. J. Chemical Approach to Positional Isomers of Glucose-Platinum Conjugates Reveals Specific Cancer Targeting Through Glucose-Transporter-Mediated Uptake *In Vitro* and *In Vivo*. *J. Am. Chem. Soc.* **2016**, *138*, 12541−12551.
(18) Mikata, Y.; Shinohara, Y.; Yoneda, K.; Nakamura, Y.; Brudziñska, I.; Tanase, T.; Kitayama, T.; Takagi, R.; Okamoto, T.; Kinoshita, I.; Doe, M.; Orvig, C.; Yano, S. Unprecedented Sugar-Dependent In Vivo Antitumor Activity of Carbohydrate-Pendant *cis*-diamminedichloroplatinum (II) Complexes. *Bioorg. Med. Chem. Lett.* **2001**, *11*, 3045−3047.
(19) Gao, X.; Liu, S.; Shi, Y.; Huang, Z.; Mi, Y.; Mi, Q.; Yang, J.; Gao, Q. Mechanistic and biological characteristics of different sugar conjugated 2-methyl malonatoplatinum(II) complexes as new tumor targeting agents. *Eur. J. Med. Chem.* **2017**, *125*, 372−384.
(20) Liu, P.; Lu, Y.; Gao, X.; Liu, R.; Zhang-Negrerie, D.; Shi, Y.; Wang, Y.; Wang, S.; Gao, Q. Highly Water-Soluble Platinum(II) Complexes as GLUT Substrates for Targeted Therapy: Improved Anticancer Efficacy and Transporter-Mediated Cytotoxic Properties. *Chem. Commun.* **2013**, *49*, 2421−2423.
(21) Liu, R.; Fu, Z.; Zhao, M.; Gao, X.; Li, H.; Mi, Q.; Liu, P.; Yang, J.; Yao, Z.; Gao, Q. GLUT1-Mediated Selective Tumor Targeting with Fluorine Containing Platinum (II) Glycoconjugates. *Oncotarget* **2017**, *8*, 39476−39496.
(22) Liu, R.; Li, H.; Gao, X.; Mi, Q.; Zhao, H.; Gao, Q. Mannose-Conjugated Platinum Complexes Reveals Effective Tumor Targeting Mediated by Glucose Transporter 1. *Biochem. Biophys. Res. Commun.* **2017**, *487*, 34−40.
(23) Li, H.; Gao, X.; Liu, R.; Wang, Y.; Zhang, M.; Fu, Z.; Mi, Y.; Wang, Y.; Yao, Z.; Gao, Q. Glucose Conjugated Platinum (II) Complex: Antitumor Superiority to Oxaliplatin, Combination Effect and Mechanism of Action. *Eur. J. Med. Chem.* **2015**, *101*, 400−408.
(24) Chen, Y.; Heeg, M. J.; Braunschweiger, P. G.; Xie, W.; Wang, P. G. A Carbohydrate-Linked Cisplatin Analogue Having Antitumor Activity. *Angew. Chem., Int. Ed. Engl.* **1999**, *38*, 1768−1769.
(25) Fuccio, C.; Spinapolice, E. G.; Ferretti, A.; Castellucci, P.; Marzola, M. C.; Trifiro, G.; Rubello, D. ^{18}F-FDG-PET/CT in Malignant Mesothelioma. *Biomed. Pharmacother.* **2013**, *67*, 539−542.
(26) Calvo, M. B.; Figueroa, A.; Pulido, E. G.; Campelo, R. G.; Aparicio, L. A. Potential Role of Sugar Transporters in Cancer and Their Relationship With Anticancer Therapy. *Int. J. Endocrinol.* **2010**, *2010*, 1−14.
(27) Kelloff, G. J.; Hoffman, J. M.; Johnson, B.; Scher, H. I.; Siegel, B. A.; Cheng, E. Y.; Cheson, B. D.; O'shaughnessy, J.; Guyton, K. Z.; Mankoff, D. A.; Shankar, L.; Larson, S. M.; Sigman, C. C.; Schilsky, R. L.; Sullivan, D. C. Progress and Promise of FDG-PET Imaging for Cancer Patient Management and Oncologic Drug Development. *Clin. Cancer Res.* **2005**, *11*, 2785−2808.
(28) Mikata, Y.; Shinohara, Y.; Yoneda, K.; Nakamura, Y.; Esaki, K.; Tanahashi, M.; Brudziñska, I.; Hirohara, S.; Yokoyama, M.; Mogami, K.; Tanase, T.; Kitayama, T.; Takashiba, K.; Nabeshima, K.; Takagi, R.; Takatani, M.; Okamoto, T.; Kinoshita, I.; Doe, M.; Hamazawa, A.; Morita, M.; Nishida, F.; Sakakibara, T.; Orvig, C.; Yano, S. Sugar-Pendant Diamines. *J. Org. Chem.* **2001**, *66*, 3783−3789.
(29) Bucher, C.; Gilmour, R. Fluorine-Directed Glycosylation. *Angew. Chem., Int. Ed. Engl.* **2010**, *49*, 8724−8728.
(30) Zhao, J.; Gou, S.; Sun, Y.; Yin, R.; Wang, Z. Nitric Oxide Donor-Based Platinum Complexes as Potential Anticancer Agents. *Chemistry* **2012**, *18*, 14276−14281.
(31) Andersson, A.; Ehrsson, H. Stability of cisplatin and its monohydrated complex in blood, plasma and ultrafiltrate - implications for quantitative analysis. *J. Pharm. Biomed. Anal.* **1995**, *13* (4−5), 639−644.
(32) Yokoo, S.; Yonezawa, A.; Masuda, S.; Fukatsu, A.; Katsura, T.; Inui, K. Differential Contribution of Organic Cation Transporters, OCT2 and MATE1, in Platinum Agent-Induced Nephrotoxicity. *Biochem.* **2007**, *74*, 477−487.

https://doi.org/10.1021/acsomega.3c06922
ACS Omega 2024, 9, 879−886